Important Heat Contribution by Tunneling Spin Scattering in Magnetic Tunnel Junction

Shuhan Liu and Shaojie Hu

State Key Laboratory for Mechanical Behavior of Materials, Center for Spintronics and Quantum Systems, School of Materials Science and Engineering, Xi'an Jiaotong University, Xi'an, Shaanxi 710049, China

We investigated the heat contribution by tunneling spin scattering of magnetic tunnel junction in parallel (P) and antiparallel (AP) states using finite element simulation. It showed a maximum temperature increase of 23.2% from P to AP, which is even more significant than the heating asymmetry caused by different current directions. A remarkable enhancement of the temperature gradient was confirmed for contributing to the extra thermal spin-transfer torque to the free layer under a specific current direction. Both the contributions of enhanced temperature and temperature gradient should be the possible reasons for the asymmetry of the critical switching current density from P to AP and AP to P. We also extended the research to a double-barrier structure, clarifying its high performance from the aspect of heat generation. Our demonstration may offer efficient tunneling magnon excitation by using the tunneling spin scattering heat.

Index Terms— **Heat contribution, spin scattering, tunneling electron.**

I. Introduction

MAGNETIC random access memory (MRAM), as a new type of nonvolatile memory device, has attracted much attention due to its unlimited endurance, high speed, and low power consumption. However, it is a great challenge to reduce the critical switching current density with higher thermal stability [1]. To overcome this issue, a series of assisted data writing processes, such as microwave-assisted switching (MAS) and thermally assisted switching (TAS), has been developed [2], [3]. Since discovering the spin caloric effects and converting heat current and spin current, a new promising method to reverse the magnetic moment has emerged by thermal spin-transfer torques [4], [5]. Both the TAS scheme and the spin-caloric effects are related to the heating process in the magnetic tunneling junction (MTJ). Therefore, it is vital to explore the production and transport of heat flow in MTJs. The impacts of Joule heating, which is the main contributor to heat in general cognition, have already been reported a lot [6]–[8]. Meanwhile, the tunneling electron scattering heat is another critical heating source caused by the inelastic scattering to excite magnons and phonons at the arrival FMs [9], [10]. Those different heating processes will make a significantly modified temperature profile in the MTJ. However, there is little consideration of the temperature and its gradient profiles induced by the tunneling spin scattering, which is the origin of the TMR effect in the MTJ. Here, we systematically studied the temperature and temperature gradient distributions induced by the tunneling spin scattering in the 3-D MTJ structure.

Manuscript received August 1, 2021; revised September 17, 2021 and October 5, 2021; accepted October 13, 2021. Date of publication October 15, 2021; date of current version March 18, 2022. Corresponding author: S. Hu (e-mail: shaojiehu@xjtu.edu.cn).

Color versions of one or more figures in this article are available at https://doi.org/10.1109/TMAG.2021.3120884.

Digital Object Identifier 10.1109/TMAG.2021.3120884

II. Method

Fig. 1(a) shows the 3-D MTJ structure, which is reported by Hayakawa *et al.* [11]. The top Au electrode size is 800 nm × 400 nm × 50 nm. The bottom SiO_2 layer size is 1600 nm × 800 nm × 50 nm. The MTJ pillar dot, 80 nm × 160 nm, is sandwiched by the top Au electrode and a SiO_2 bottom substrate. Fig. 1(b) shows the crossing section of MTJ structure, which consists of Ta (5)/Ru (50)/Ta (5)/NiFe (5)/MnIr (8)/CoFe (4)/Ru (0.8)/CoFeB (5)/MgO (1.5)/CoFeB (2)/Ta (5)/Ru (5) (all in nanometers). To ensure the high calculation accuracy for the thin layers, we created the swept meshes on the MTJ layers in 3-D sweeping the mesh from the source face along with the domain to an opposite destination face in COMSOL. The element size is calibrated by using the general physics model with the extra fine method. The minimum mesh size of the junction stack is 0.32 nm, which is much smaller than the thickness of MTJ layers.

In the early report, 1-D simulations were conducted using a numerical finite difference method to solve the heat equation [10]

$$C_p d\frac{\partial T}{\partial t} - K\left(\frac{\partial^2 T}{\partial x^2}\right) = \rho j^2 + \frac{jV}{l}\exp\left(-\frac{x}{l}\right) \tag{1}$$

where C_p is the heat capacity, d is the mass density, T is the temperature, t is the time, K is the heat conductivity, ρ is the electrical resistivity, j is the current density, V is the voltage drop across the tunnel barrier, l is the electron inelastic scattering mean free path, and x is the position in the stack. The heat generation of MTJs generally contains both the Joule heating in metal layers [the first term on the right in (1)] and the tunneling spin scattering heating in the electrode where the tunneling electrons arrive [the second term on the right in (1)].

In fact, the electron transport through the tunneling barrier is ballistic transport. It should be elastic scattering in the tunneling barrier [12]. Thus, there should be no or less energy loss

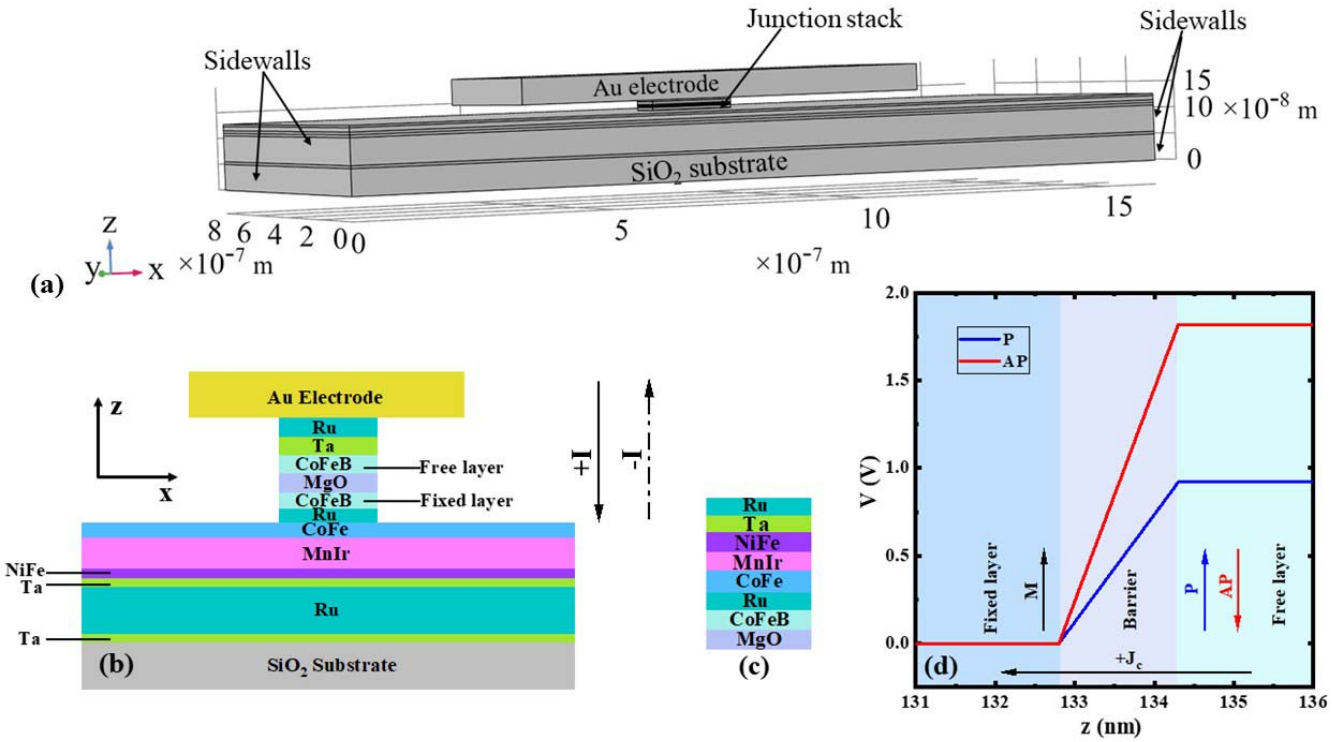

Fig. 1. (a) Geometry and boundary condition of 3-D simulation. (b) Structure of the MgO-based MTJ. (c) Additional part for DMTJ. (d) Voltage drop in P and AP states for the MgO barrier.

when the electron is crossing the barrier. However, the spin-dependent scattering of electrons in the arrival ferromagnetic layer leads to a loss of energy and the change of momentum due to the electron–electron scattering, phonon scattering, and magnon scattering. The released energy will excite hot electrons, magnons, and phonons of the arrival electrode, leading to a temperature rise macroscopically. Therefore, the Joule heating contribution in the tunneling barrier layer should be negligibly small. In our simulation, the tunneling spin scattering heat occurs in the ferromagnet layer rather than the barrier. We remove the Joule heating contribution in the MgO layer and add the spin scattering heating term in the electron arrival ferromagnetic layer. Moreover, the scattering process is directly related to the magnetic states of P or AP. We have to discuss the tunneling spin scattering heat in these two states. Then, the heat equation in 3-D structure will be modified as follows:

$$C_p d\frac{\partial T}{\partial t} - K\left(\frac{\partial^2 T}{\partial x^2} + \frac{\partial^2 T}{\partial y^2} + \frac{\partial^2 T}{\partial z^2}\right) = \rho\left(j_x^2 + j_y^2 + j_z^2\right) + \frac{j_z \times V_{P(\mathrm{AP})}}{l}\exp\left(-\frac{|z - z_0|}{l}\right) \quad (2)$$

where V_{P} and V_{AP} can be further expressed by the resistivity of MgO and the TMR ratio: $V_P = j_z \times \rho_P \times h$ and $V_{\mathrm{AP}} = j_z \times \rho_P \times h \times (\mathrm{TMR} + 1)$. h is the thickness of tunneling barrier. The values of ρ_P and TMR ratio in our simulation are 7.85 $\Omega \cdot$ m and 90%, respectively, calculated from the R–H curve in the literature reported by Hayakawa *et al.* [11]. z in the exponential term should be the position in the stack on the z-axis. Since the tunneling process in the 3-D structure occurs along the z-axis direction, z_0 represents the z-coordinate of upper and lower surfaces of the tunneling barrier under positive and negative current directions, respectively. The current following from the top Au electrode to the bottom is defined as the positive current $(+I)$, while the current flowing from the bottom to the top is defined as the negative current $(-I)$, as shown in Fig. 1(b). For a positive current, the value of z_0 is taken as 134.3 nm, while under a negative current z_0 is 132.8 nm. Since the spin-dependent transport of electrons in MTJ is critical to the TMR ratio, the electron inelastic scattering mean free path should correspond to the electron spin-dependent scattering length in the ferromagnet. The electron inelastic scattering mean free path (l) value is assumed as 2 nm in our simulation based on the previous reports [13], which is almost corresponding to the spin scattering length in the ferromagnetic layer. It should be noted that the removed Joule heating term $-((j_z \times V_{\mathrm{P(AP)}})/h)$ only occurs on the tunnel barrier layer, and the spin scattering heat term $((j_z \times V_{P(\mathrm{AP})})/l)\exp(-((|z - z_0|)/l))$ only occurs in the ferromagnetic layer closed the barrier.

In our simulation, all parameters of the related materials are listed in Table I [10], [14]. Due to the fast surface heating exchange, the surface temperature of the far sidewalls was all assumed to be fixed at 300 K, as shown in Fig. 1(a). The other setting of boundary condition is similar to that reported by Prejbeanu *et al.* [3]. Finally, we study it using a stationary solver with a constant current source in the device.

III. Results and Discussion

Suppose that we set positive current flows from the top to the bottom. The different voltage drops are apparently obtained for parallel and antiparallel states in Fig. 1(d), where the

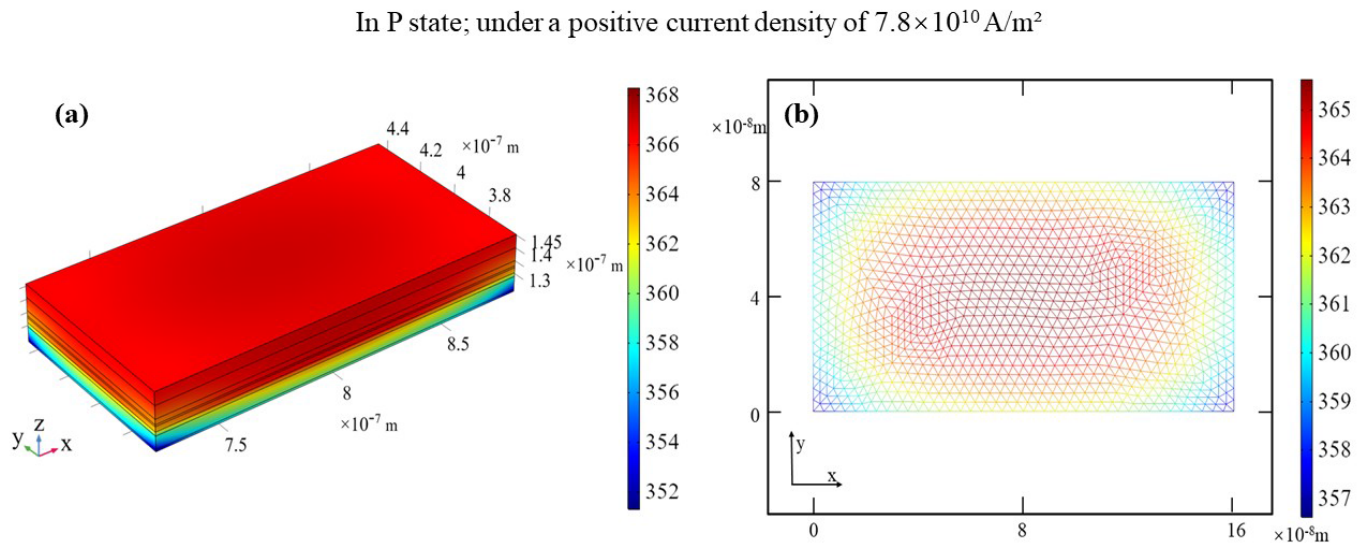

Fig. 2. (a) 3-D temperature distribution of the MTJ stack with a positive current of 1 mA in the P state. (b) xy plane temperature distribution with the mesh nets in the fixed ferromagnetic layer.

TABLE I

PARAMETERS OF MATERIALS USED IN SIMULATION

Element	C_p (J/(kg · K))	K (W/m · K)	d (g/cm^3)	ρ ($\mu\Omega$ · cm)
Au	126	237	19.3	2.2
Ru	243	116	12.3	7.2
Ta	139	58	16.6	154
CoFeB	421	100	8.9	6.25
MgO	30	877	3.58	7850(P) 15531(AP)
CoFe	421	100	8.9	6.25
MnIr	409	35.6	10.3	147
NiFe	401	88	8.7	18
SiO_2	700	1.4	2.2	-

voltage drop in the AP state is almost twice that in the P state. Such a huge difference is a typical embodiment of the TMR effect in the MTJ due to the significant tunneling spin scattering. It is obvious that different tunneling spin scatterings will significantly distinguish the temperature profiles for AP and P states based on (2). As reported in the previous literature, the tunneling electron scattering is related to the current direction [12]. Therefore, it may help us clear all the heating contributions in the MTJ for AP and P states with two current directions.

Fig. 2(a) shows the 3-D temperature distribution of MTJ with a positive current of 1 mA in the P state. The temperature distribution is not uniform due to the 3-D heat dispersion. Such 3-D simulation results could help us to understand the temperature profiles in real devices, which could not be realized by only using the 1-D simulation. To clear the in-plane temperature profile, we cut the xy plane at $z = 130.8$ nm (in fixed ferromagnetic layer and 2 nm from the barrier surface) and plot the temperature profile with mesh nets shown in Fig. 2(b). The in-plane temperature is symmetrically distributed with the center. Thus, the generation of thermal spin current is negligible by the in-plane temperature gradient. The temperature profile in the z-direction is most crucial for the thermally driven spin injection effect.

TABLE II

VALUES OF T_{Max} AND α

Configuration	*P+*	*AP+*	*P-*	*AP-*
T_{Max}(K)	368.263	435.104	395.240	488.489
α (mA^2/K)	68.26	135.03	96.24	188.45

To evaluate the temperature profile in the z-direction in a simple way, we only show the temperature for the four kinds of configurations at the center of the pillar, as shown in Fig. 3(a). It is clear that the heat center relates to the current direction because of the different tunneling directions of electron scattering in the arriving electrodes. The temperature distribution tendency in the z-direction is consistent with the previous 1-D model results. At the same time, it also makes the absolute temperature difference at the same states (P or AP), which mainly arises from the distinction of heat dissipation for the arriving probes. In addition, all the temperature in the AP state is much higher than that in the P state. To further understand this feature, we also plotted the current dependence curve of the maximum temperature in the z-direction, as shown in Fig. 3(b). It is obvious that the value of tunneling spin scattering heat still follows the law proportional to the square of the current, which is consistent with the Joule heating. Then, we fit the T-I curves using the equation $T = \alpha I^2 + T_0$ to obtain the coefficient α for four configurations. For intuitively comparing, the maximum T at current $I = 1$ mA (current density: 7.8×10^{10} A/m^2) and the coefficient α are listed in Table II for the four configurations.

Under different combinations of current direction and magnetic state, the temperature increases to 23.2% from P− to AP−. This is even more significant than that caused by the different current directions, which raises most by 13.5%. We can also see that the maximum value of coefficient α in the P state is still lower than the minimum value of the AP state. It is strong evidence that the tunneling spin scattering dominates the heat contribution in MTJ. Also, the ratio of α for AP and P states is about 1.9, which is consistent with TMR+1. This indicates that the higher TMR will contribute

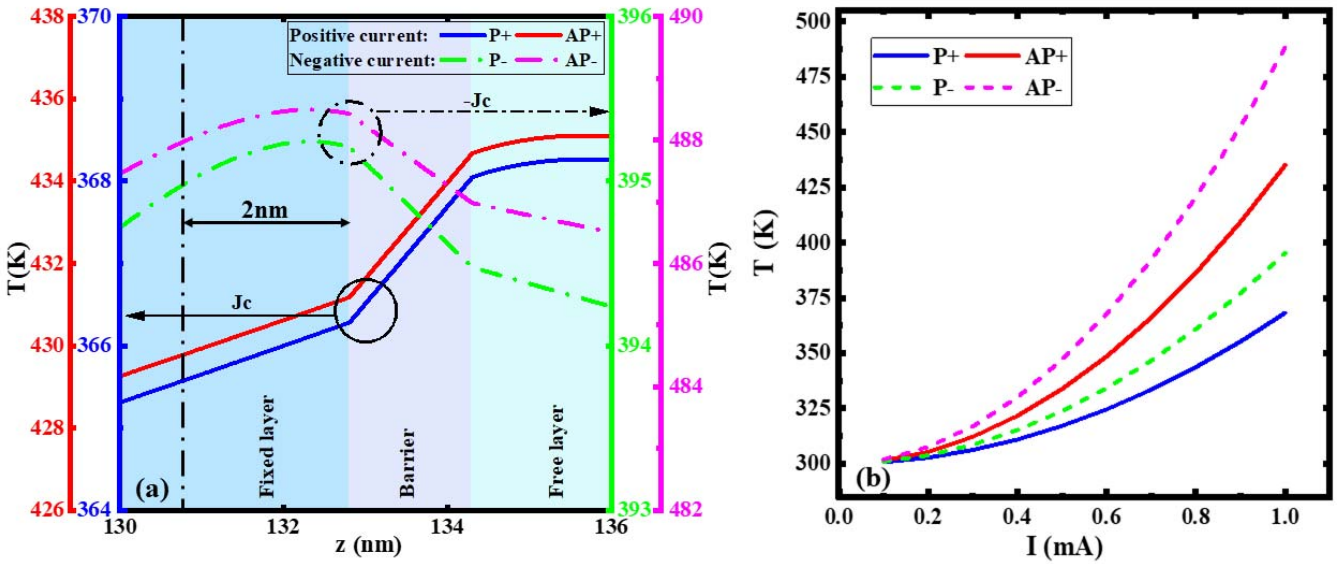

Fig. 3. (a) Temperature distribution on the z-axis (along the tunneling direction) with 1 mA current for four kinds of configurations. (b) Maximum temperature as a function of bias current in the MTJ for four different combinations of magnetization directions and current directions.

much more tunneling spin scattering heat. The temperature difference ($\Delta T_{AP^- -> P^+}$) for AP− to P+ is calculated to be 120.19 I^2 based on the corresponding coefficient α. The temperature difference will reach 120 K for the current density of 7.8×10^{10} A/m^2. Such a significant temperature difference indicates a lower switching current density from AP to P states due to TAS. Therefore, the tunneling spin scattering should be considered as the main reason for the asymmetric switching current density from AP to P and P to AP in most experiment results.

Moreover, another characteristic of tunneling spin scattering heat is that it is generated locally at the arrival ferromagnetic layer, where the temperature gradient in the z-direction will be significantly modified. To understand the influence of the temperature gradient profiles, we plotted the temperature gradient distribution for four configurations in Fig. 4(a). There is a significant influence on the sign of temperature gradient around the barrier by current direction, which is quite different from the case only considering Joule heating. For the positive current, the sign of temperature gradient reverses at the free layer. For the negative current, the reversed sign of temperature gradient appears in the fixed layer. The temperature extremum is the transition point, which is about 1.3 and 0.5 nm from the MgO barrier edge for free and fixed layers, respectively. To gain the thermal spin-transfer torque contribution on the free layer, we calculate the thermal spin voltage ($V_s = S_s \nabla T \lambda_{CFB}$) by using the spin-dependent Seebeck effect in the fixed layer, which is the main contributor of the thermal spin-transfer torque to the free layer [15]–[17]. S_s is about 60 μV/K [18]. We assume that the spin scattering length λ_{CFB} is 2 nm in the CFB layer. The temperature gradient is not constant in the fixed layer for the negative current. Thus, we use the temperature difference (ΔT) between the lower interface of the MgO barrier and the position 2 nm away from the interface to get the value of $\nabla T \lambda_{CFB}$. The related position is marked by the black dotted-dashed line in Fig. 4(a). Thus, the thermal spin voltage can be calculated by using the obtained ΔT. The functions of the thermal spin voltage with bias current under four configurations are plotted in Fig. 4(b). In addition, all thermal spin voltages are more significant for the positive current than that for the negative current both in P and AP states. The unique feature indicates that the current direction is the main dominator for enhancing the thermal spin-transfer torque contribution.

As we know, the tunneling barrier plays a decisive role in tunneling spin scattering, which is the origin of TMR and spin scattering heat. Thus, the use of a multi-barrier structure is expected to obtain the efficient spin scattering effect. The double-barrier magnetic tunnel junction (DMTJ), as one of the representatives of multi-barrier structure, has been widely studied recently because of the improved TMR and low critical switching current density [19]–[24].

To gain insight into the tunneling spin scattering heat effect in DMTJ, we studied the temperature and temperature gradient profiles by comparing them with a single-barrier magnetic tunnel junction (SMTJ). Here, the stack of DMTJ was obtained from the SMTJ by adding another MgO (1.5)/CoFeB (5)/Ru (0.8)/CoFe (4)/MnIr (8)/NiFe (5)/Ta (5)/Ru (5) (all in nanometers) on the top of CoFeB free layer, as shown in Fig. 1(c). In order to make a fair comparison, we used the same TMR ratio (90%) for the DMTJ and SMTJ. The RA is a bit different for the SMTJ and DMTJ. Based on the Sato *et al.*'s [25] report, here, the RAs are 10 and 12 $\Omega \cdot \mu$m^2 for the SMTJ and DMTJ, respectively. To simplify, we only compare the results of the parallel state with the positive current density 7.8×10^{10} A/m^2, as shown in Fig. 5(a) and (b). The temperature is much higher in DMTJ than that in SMTJ. Since the higher temperature could reduce thermal stability, the TAS will be much more efficient in the DMTJ. In addition, the temperature gradient profiles are also plotted in Fig. 5(c) and (d). The temperature gradient in fixed and CoFeB (closed top barrier) layers has the same sign for DMTJ. The thermal spin transfer-torque effect will be enhanced in the DMTJ and suppressed in SMTJ. The thermal spin voltage is evaluated

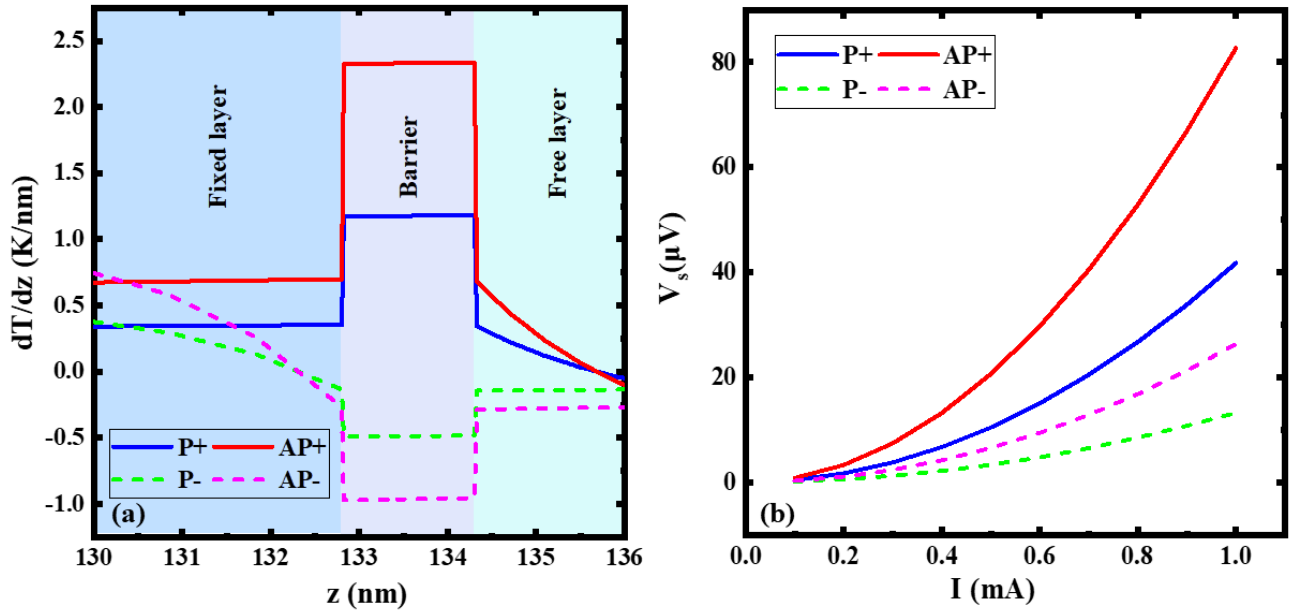

Fig. 4. (a) Temperature gradient distribution on the z-axis (along the tunneling direction) with a current density of 7.8×10^{10} A/m^2 for various configurations. (b) Thermal spin voltage as a function of bias current in the fixed layer for four different combinations of magnetization directions and current directions.

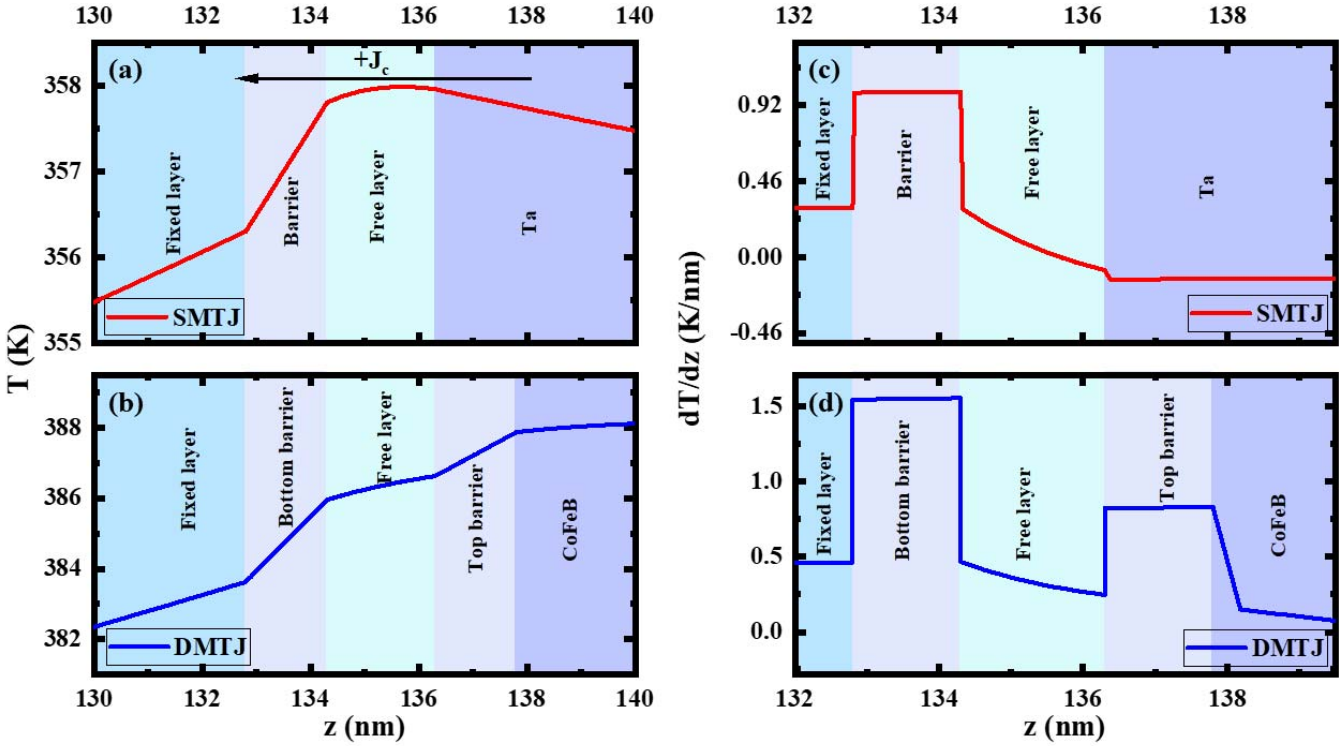

Fig. 5. Temperature distribution on the z-axis for (a) SMTJ and (b) DMTJ. The horizontal black arrow represents the current direction, while the vertical arrow represents the magnetization direction. The temperature gradient distribution for (c) SMTJ and (d) DMTJ with a positive current density of 7.8×10^{10} A/m^2.

as 65.5 and 23.0 μV for DMTJ and SMTJ, respectively. This phenomenon is in good agreement with the conclusion that the thermal spin effect gets enhanced in DMTJ predicted by Jia *et al.* [26].

IV. Conclusion

Based on the systematic study of tunneling spin scattering heat, we have proposed the other kind of heat asymmetry caused by the magnetization direction states of AP or P and confirmed its significant contribution to both temperature and temperature gradient. This heat source has a non-ignorable impact on the thermal stability and the critical switching current density of MTJ, making it extremely important to the design of spintronics devices. In addition, our demonstration has also shown that the tunneling spin scattering heat may greatly enhance thermal spin injection, thereby offering another effective thermally assisted magnetic switching scheme.

ACKNOWLEDGMENT

This work is partially supported by the National Key Research Program of China (Grant No. 2017YFA0206200), National Natural Science Foundation for Young Scholar of China (Grant No. 51601139), International Postdoctoral Exchange Fellowship Program (Grant No. 20190083) and Natural Science Foundation of Shaanxi Province (Grant No. 2021JM-022).

REFERENCES

[1] S. Ikeda *et al.*, "Magnetic tunnel junctions for spintronic memories and beyond," *IEEE Trans. Electron Devices*, vol. 54, no. 5, pp. 991–1002, May 2007.

[2] C. Thirion, W. Wernsdorfr, and D. Mailly, "Switching of magnetization by nonlinear resonance studied in single nanoparticles," *Nature Mater.*, vol. 2, pp. 524–527, Jul. 2003.

[3] I. L. Prejbeanu *et al.*, "Thermally assisted MRAM," *J. Phys., Condens. Matter*, vol. 19, no. 16, 2007, Art. no. 165218.

[4] O. Gomonay, K. Yamamoto, and J. Sinova, "Spin caloric effects in antiferromagnets assisted by an external spin current," *J. Phys. D, Appl. Phys.*, vol. 51, no. 26, Jul. 2018, Art. no. 264004.

[5] M. Hatami, G. E. W. Bauer, Q. Zhang, and P. J. Kelly, "Thermal spin-transfer torque in magnetoelectronic devices," *Phys. Rev. Lett.*, vol. 99, no. 6, 2007, Art. no. 066603.

[6] D. H. Lee and S. H. Lim, "Increase of temperature due to Joule heating during current-induced magnetization switching of an MgO-based magnetic tunnel junction," *Appl. Phys. Lett.*, vol. 92, no. 23, 2008, Art. no. 233502.

[7] N. Strelkov *et al.*, "Impact of Joule heating on the stability phase diagrams of perpendicular magnetic tunnel junctions," *Phys. Rev. B, Condens. Matter*, vol. 98, no. 21, Dec. 2018, Art. no. 214410.

[8] S. Hu and T. Kimura, "Significant modulation of electrical spin accumulation by efficient thermal spin injection," *Phys. Rev. B, Condens. Matter*, vol. 90, no. 13, Oct. 2014, Art. no. 134412.

[9] S. Zhang, P. M. Levy, A. C. Marley, and S. S. P. Parkin, "Quenching of magnetoresistance by hot electrons in magnetic tunnel junctions," *Phys. Rev. Lett.*, vol. 79, no. 19, p. 3744, 1997.

[10] R. C. Sousa *et al.*, "Tunneling hot spots and heating in magnetic tunnel junctions," *J. Appl. Phys.*, vol. 95, no. 11, pp. 6783–6785, 2004.

[11] J. Hayakawa *et al.*, "Current-induced magnetization switching in MgO barrier based magnetic tunnel junctions with CoFeB/Ru/CoFeB synthetic ferrimagnetic free layer," *Jpn. J. Appl. Phys.*, vol. 45, no. 40, pp. L1057–L1060, Oct. 2006.

[12] E. Gapihan *et al.*, "Heating asymmetry induced by tunneling current flow in magnetic tunnel junctions," *Appl. Phys. Lett.*, vol. 100, no. 20, May 2012, Art. no. 202410.

[13] A. Jablonski, P. Mrozek, G. Gergely, M. Menhyárd, and A. Sulyok, "The inelastic mean free path of electrons in some semiconductor compounds and metals," *Surf. Interface Anal.*, vol. 6, no. 6, pp. 291–294, Dec. 1984.

[14] *MatWeb*. Accessed: Jun. 2020. [Online]. Available: http://www.matweb.com

[15] A. Slachter, F. L. Bakker, J.-P. Adam, and B. J. van Wees, "Thermally driven spin injection from a ferromagnet into a non-magnetic metal," *Nature Phys.*, vol. 6, no. 11, pp. 879–882, Nov. 2010.

[16] R. Jansen, A. M. Deac, H. Saito, and S. Yuasa, "Thermal spin current and magnetothermopower by Seebeck spin tunneling," *Phys. Rev. B, Condens. Matter*, vol. 85, no. 9, Mar. 2012, Art. no. 094401.

[17] S. Hu, H. Itoh, and T. Kimura, "Efficient thermal spin injection using CoFeAl nanowire," *NPG Asia Mater.*, vol. 6, no. 9, p. e127, Sep. 2014.

[18] N. Liebing *et al.*, "Determination of spin-dependent Seebeck coefficients of CoFeB/MgO/CoFeB magnetic tunnel junction nanopillars," *J. Appl. Phys.*, vol. 111, no. 7, Apr. 2012, Art. no. 07C520.

[19] J. Barnaś and A. Fert, "Magnetoresistance oscillations due to charging effects in double ferromagnetic tunnel junctions," *Phys. Rev. Lett.*, vol. 80, no. 5, p. 1058, 1998.

[20] M. Watanabe, J. Okabayashi, H. Toyao, T. Yamaguchi, and J. Yoshino, "Current-driven magnetization reversal at extremely low threshold current density in (Ga,Mn)As-based double-barrier magnetic tunnel junctions," *Appl. Phys. Lett.*, vol. 92, no. 8, Feb. 2008, Art. no. 082506.

[21] A. G. Petukhov, A. N. Chantis, and D. O. Demchenko, "Resonant enhancement of tunneling magnetoresistance in double-barrier magnetic heterostructures," *Phys. Rev. Lett.*, vol. 89, no. 10, Aug. 2002, Art. no. 107205.

[22] A. Vedyayev, N. Ryzhanova, B. Dieny, and N. Strelkov, "Resonant spin-torque in double barrier magnetic tunnel junctions," *Phys. Lett. A*, vol. 355, no. 3, pp. 243–246, Jul. 2006.

[23] I. Theodonis, A. Kalitsov, and N. Kioussis, "Enhancing spin-transfer torque through the proximity of quantum well states," *Phys. Rev. B, Condens. Matter*, vol. 76, no. 22, Dec. 2007, Art. no. 224406.

[24] J. Peralta-Ramos, A. M. Llois, I. Rungger, and S. Sanvito, "I–V curves of Fe/MgO (001) single- and double-barrier tunnel junctions," *Phys. Rev. B, Condens. Matter*, vol. 78, no. 2, Jul. 2008, Art. no. 024430.

[25] H. Sato *et al.*, "Comprehensive study of CoFeB-MgO magnetic tunnel junction characteristics with single- and double-interface scaling down to 1X nm," in *IEDM Tech. Dig.*, Dec. 2013, pp. 3.2.1–3.2.4.

[26] X. Jia, S. Wang, and M. Qin, "Enhanced thermal spin transfer in MgO-based double-barrier tunnel junctions," *New J. Phys.*, vol. 18, no. 6, Jun. 2016, Art. no. 063012.